BIOCHEMISTRY
including biophysical chemistry & molecular biology

Article

pubs.acs.org/biochemistry

RNA Binds to Tau Fibrils and Sustains Template-Assisted Growth

Paul D. Dinkel, Michael R. Holden, Nadira Matin, and Martin Margittai*

Department of Chemistry and Biochemistry, University of Denver, Denver, Colorado 80208, United States

Supporting Information

ABSTRACT: Tau fibrils are the main proteinacious components of neurofibrillary lesions in Alzheimer disease. Although RNA molecules are sequestered into these lesions, their relationship to Tau fibrils is only poorly understood. Such understanding, however, is important, as short fibrils can transfer between neurons and nonproteinacious factors including RNA could play a defining role in modulating the latter process. Here, we used sedimentation assays combined with electron paramagnetic resonance (EPR), fluorescence, and absorbance spectroscopy to determine the effects of RNA on Tau fibril structure and growth. We observe that, in the presence of RNA, three-repeat (3R) and four-repeat (4R) Tau form fibrils with parallel, in-register arrangement of β-strands and exhibit an asymmetric seeding barrier in which 4R Tau grows onto 3R Tau seeds but not vice versa. These structural features are similar to those previously observed for heparin-induced fibrils, indicating that basic conformational properties are conserved, despite their being molecular differences of the nucleating agents. Furthermore, RNA sustains template-assisted growth and binds to the fibril surface and can be exchanged by heparin. These findings suggest that, in addition to mediating fibrillization, cofactors decorating the surface of Tau fibrils may modulate biological interactions and thereby influence the spreading of Tau pathology in the human brain.

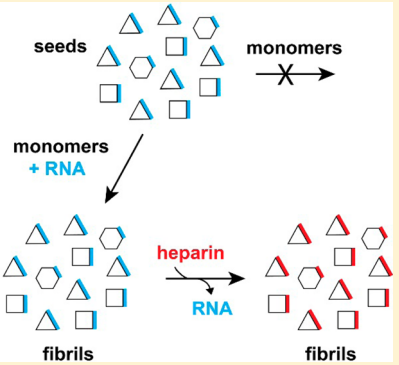

Intracellular lesions in Alzheimer disease brain are characterized by neurofibrillary tangles in cell bodies, neuropil threads in cytoplasmic processes, and dystrophic neurites around senile plaques.[1] All of these lesions contain Tau fibrils. Recent evidence suggests that the progression of Tau pathology[2,3] could be based on the cell-to-cell transfer of Tau aggregates via axonally connected neurons.[4−6] Once taken up by recipient cells, Tau fibrils are thought to recruit native, unfolded Tau proteins in a process of template-assisted conversion.[7] The molecular mechanism of this process is poorly understood.

Adult human brain expresses six different Tau isoforms, ranging in size from 352 to 441 amino acids, all of which are deposited in the brains of Alzheimer disease patients.[8] The isoforms can be divided into three-repeat (3R) Tau and four-repeat (4R) Tau based on the number of microtubule binding repeats present.[9] The repeats are 31 to 32 amino acids in length and together constitute the protease-resistant core of the fibril.[10−12] The remaining N- and C-terminal residues comprise a fuzzy, unstructured coat[13] that protrudes from the fibril core.[14] Removal of these regions results in the truncated Tau constructs K18 (4R) and K19 (3R)[15] that show greatly accelerated aggregation kinetics.[16] Presumably, the N- and C-termini fold back onto the repeat region,[17] preventing self-assembly. Both truncated and full-length Tau form fibrils with an amyloid-type cross-β structure, in which β-strands extend perpendicular to the long fibril axis and are spaced ∼4.7 Å apart.[18,19]

Fibril assembly is initiated by a critical nucleation step in which multiple Tau molecules join into a propagation-competent structure.[20] This step is facilitated by negatively charged cofactors such as heparin,[21,22] fatty acids,[23,24] and RNA[25,26] that act to counter the positive charge within the repeat region of Tau. In the absence of cofactors, Tau does not aggregate unless it is used at concentrations far exceeding cellular levels and subjected to extremes of pH, temperature, or ionic strength.[27,28]

It is currently unknown what events initiate Tau fibrillization in the cell. Phosphorylation of Tau increases the soluble pool of the protein based on its lowered affinity to microtubules.[29−32] However, whether phosphorylation alone is sufficient to induce fibrillization remains unresolved. Additional cellular factors, including those that are applied *in vitro*, could play a critical role. Although RNA was found to stimulate Tau aggregation, compared to other cofactors, its effects on fibril formation are still poorly understood. Also, despite being sequestered into the fibrillar lesions of Tau in Alzheimer disease[33] and other tauopathies,[34] it remains unclear whether RNA binds to fibrils. Here, we investigated the formation of Tau fibrils in the presence of RNA. Our findings provide insights into fibril structure and propagation that could have important implications for the spreading of Tau pathology.

MATERIALS AND METHODS

Expression and Purification of Tau. Tau constructs K18 and K19 (in pET28) with their natural cysteines replaced by

Received: April 24, 2015
Revised: July 15, 2015
Published: July 15, 2015

DOI: 10.1021/acs.biochem.5b00453
Biochemistry 2015, 54, 4731−4740

serines and single cysteines introduced at positions 309, 310, 311, 317, 322, and 326 were expressed and purified as previously described.[35] Briefly, BL21 (DE3) competent cells (Agilent) transformed with the appropriate pET28 vectors were grown at 37 °C to an OD_{600} of 0.8−1.0. Expression was induced with 1 mM isopropyl β-D-1-thiogalactopyranoside, and cells were incubated for 3 1/2 h at 37 °C. The bacteria were then centrifuged at 3000*g* for 15 min, and pellets were resuspended in 500 mM NaCl, 20 mM PIPES (J.T. Baker), 5 mM EDTA, 50 mM 2-mercaptoethanol, pH 6.5, buffer. Bacterial samples were stored at −80 °C until further use. For purification, bacteria were heated to 80 °C for 20 min, cooled on ice for 5 min, lysed by 1 min of sonication, and pelleted at 15 000*g* for 30 min. Tau-containing supernatants were precipitated with a 55% w/v addition of ammonium sulfate. Samples were rocked at 25 °C for 1 h and then centrifuged at 15 000*g* for 10 min. Protein pellets were resuspended in dH_2O containing 4 mM dithiothreitol (DTT), sonicated for 40 s, and syringe-filtered (0.45 μm Acrodisc GxF/GHP filter (Pall Life Sciences)). The samples were then loaded onto a Mono S 10/100GL column (GE Healthcare) and eluted with a linear 50 mM to 1 M NaCl gradient. Fractions were analyzed by SDS-PAGE. Pooled samples were further purified on a Superdex 200 size exclusion column (GE Healthcare) using the following elution buffer: 100 mM NaCl, 1 mM EDTA, 2 mM DTT, and 20 mM Tris at pH 7.4. Monomeric Tau was precipitated overnight at 4 °C with the addition of a 4-fold volumetric excess of acetone containing 5 mM DTT. Precipitated Tau was sedimented, washed with acetone (2 mM DTT), and stored at −80 °C.

Spin Labeling of Tau Monomer. Precipitated Tau pellets were dissolved in 200−400 μL of 8 M guanidine hydrochloride. A ∼10-fold molar excess of [1-oxyl-2,2,5,5-tetramethyl-Δ3-pyrroline-3-methyl] methanethiosulfonate (MTSL) spin label (Toronto Research Chemicals, Downsview, Canada) was added to Tau and allowed to incubate for at least 1 h. Tau samples were then purified with a PD-10 column (GE Healthcare) to remove denaturant and unreacted spin label. The elution buffer consisted of 10 mM HEPES, (J.T. Baker) at pH 7.4 and 100 mM NaCl. Concentrations of Tau monomers were determined using the BCA method (Thermo Scientific).

EPR Measurements of Fibrils. Fibrils were formed by incubating 35 μM spin-labeled Tau and 70 μg/mL polyA RNA (Sigma P9403) for 3 days with stirring in 100 mM NaCl, 10 mM HEPES buffer at pH 7.4. The RNA was polydisperse (ranging in size from ∼0.2 to 2 kb), as judged by agarose gel electrophoresis. Fibrils were also prepared with 30−65 μM spin-labeled Tau with polyU (Sigma P9528), double-stranded polyAU (Sigma P1537), tRNA (Sigma R8759), or RNA extract from baker's yeast (Sigma R650) at concentration ranges of 140−200 μg/mL or with polydA (Sigma P0887) at 36 μg/mL. Additionally, assembly was performed with a 4-fold molar excess of polyglutamate (Sigma P1943) or with double-stranded DNA, circular (pET28) or linear (Sigma D4522), at 100−200 μg/mL. Notably, in both cases, double-stranded DNA failed to properly induce fibrillization. Fibrils were pelleted at >100 000*g* for 30 min. Pellets were washed with buffer, centrifuged further for 10 min, and transferred to 0.60 mm i.d. × 0.84 mm o.d. borosilicate capillaries (VitroCom CV6084-100). Samples were measured by a Bruker EMX spectrometer fitted with an ER 4119HS resonator using a 12 mW incident microwave power and 150 G scan width. Spectra were normalized according to the total number of spins using double integration. A minor background that resulted from Tau monomers (<2.0 mol %) was subtracted from all spectra.

Seeding Kinetics. Tau-seeded aggregation was monitored using an acrylodan fluorescence assay previously described.[36] Fibril seeds were prepared by incubating 25 μM K18 or K19 with 50 μg/mL of polyA RNA in 100 mM NaCl, 10 mM HEPES, pH 7.4, buffer for 3 days with stirring. Fibrils were cooled on ice for 15 min and continuously sonicated for 20 s at power setting 3 in a Fisher Scientific Sonifier (150 Series) to induce fibril breakage. Fragmented fibril seeds (10% monomer equivalents) were added to 10 μM K18 or K19 monomer to initiate aggregation. Monomer included 98% cysteine-free Tau (cysteines replaced with serines) and 2% Tau labeled at cysteine 310. Reactions included the addition of 20 μg/mL polyA RNA. Aggregation kinetics were measured using a Fluorolog 3 fluorometer (HORIBA Jobin Yvon). The excitation wavelength was set at 360 nm, and emission spectra were collected from 400 to 600 nm. The excitation and emission slit widths in these experiments were 5 nm. To depict seeded growth, the inverse of the emission maxima were plotted as a function of time.

Successive Seeding. Successive seeding reactions were carried out with and without the addition of polyA RNA as a cofactor. Initial reactions (1.4 mL) contained 25 μM K18 or K19 WT, 125 μg/mL RNA, and 10% seeds (monomer equivalents). Reactions proceeded for 24 h. Five hundred microliters was removed, sonicated on ice, and used to provide fibril seeds for the following reaction. Each additional reaction (25 μM Tau monomer) was seeded with 10% seeds (monomer equivalents) from the previous reaction and was incubated for 24 h with or without 125 μg/mL polyA RNA. Fibrils from each reaction were centrifuged at >100 000*g* for 30 min. Pellets were washed with buffer (100 mM NaCl, 10 mM HEPES, pH 7.4), centrifuged again for 10 min, taken up in 1× sample buffer (62.5 mM Tris, pH 6.8, 4% SDS, 10% sucrose, 5% 2-mercaptoethanol, 0.001% bromophenol blue), and analyzed by SDS-PAGE. Where appropriate, bands were quantified by ImageJ.

RNA Binding to Tau Fibrils and Exchange with Heparin. Tau/RNA fibril seeds were prepared as described under Seeding Kinetics. Ten percent seeds (monomer equivalents) was added to 25 μM K18 or K19 monomer with 50 μg/mL polyA RNA in 100 mM NaCl, 10 mM HEPES, pH 7.4, buffer. Samples were inverted three times and incubated at 37 °C for 2 h. Fibrils were centrifuged at >100 000*g* for 30 min, and pellets were dissolved in 60 μL of 2% w/v sodium dodecyl sulfate. To supernatants was added 60 μL of 2% w/v sodium dodecyl sulfate, and both pellets and supernatants were brought to 1250 μL with buffer. RNA contained in pellets was determined at Abs_{260} using a Cary 100 Bio UV−visible spectrophotometer. In heparin exchange experiments, fibrils were formed with RNA and K18 or K19 Tau as before. Heparin (average MW = 4400, Celsus, EN-3225) or fluorescently conjugated heparin (average MW = 18 000, Invitrogen, H7482) was then added for final concentrations of 50 and 2.5 μM, respectively. On the basis of the RNA size distribution (0.2−2 kb), these concentrations corresponded to a ∼66−660-fold molar excess of Celsus-heparin over RNA and a ∼3.3−33-fold molar excess of Invitrogen-heparin over RNA. It is likely that the molecular weight of heparin affects its binding affinity to Tau fibrils, with higher molecular weight species exhibiting increased affinity. However, since heparin is also inherently heterogeneous (the commercial forms are isolated from porcine

DOI: 10.1021/acs.biochem.5b00453
Biochemistry 2015, 54, 4731−4740

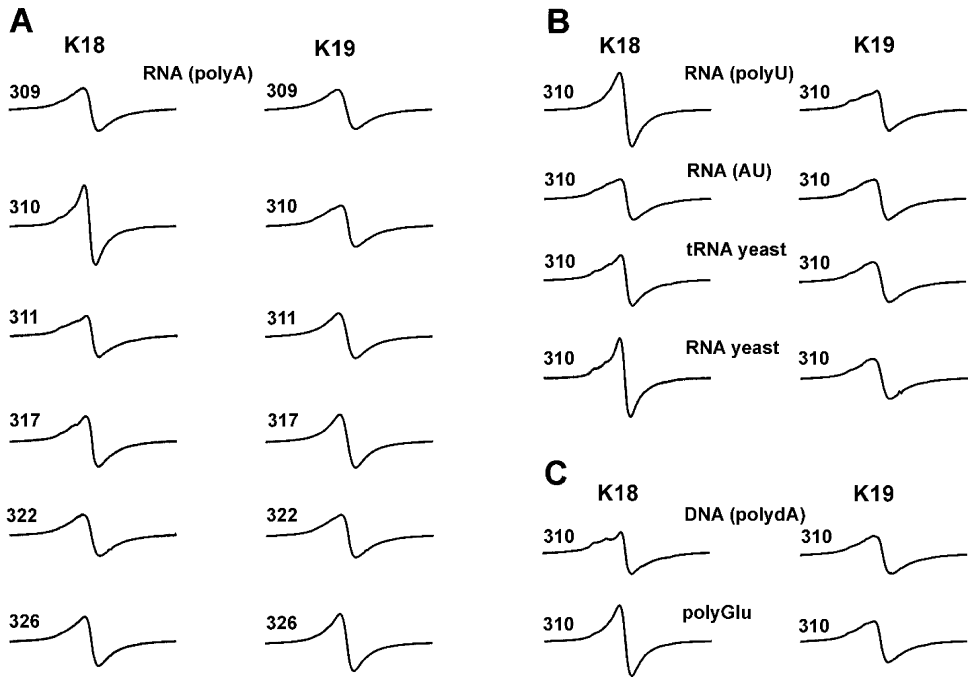

Figure 1. EPR analysis of Tau fibrils. Single cysteines in K18 and K19 monomers were spin-labeled with the nitroxide label MTSL and allowed to fibrillize in the presence of polyanionic cofactors. All spectra were taken at 150 G and normalized to the same number of spins. K18 and K19 fibrils were formed in the presence of (A) polyA, (B) polyU, polyAU, tRNA, and yeast RNA extract, and (C) polydA and polyGlu. The single-line EPR spectra observed for all fibrils indicate that, regardless of cofactor, β-strands in the proteins are aligned parallel and in-register.

intestinal mucosa), the specific sugar composition and the particular pattern of sulfonation will affect fibril binding as well. Similar arguments will apply for binding of Tau fibrils to heparan sulfate proteoglycans on the cell surface (see Discussion). Samples were inverted five times and incubated 24 h at 37 °C. Subsequently, fibrils were sedimented and resuspended as before. Absorbance of fluorescent heparin was determined in both pellet and supernatant at 490 nm. RNA present was determined by absorbance at 260 nm, with minor contributions from fluorescent heparin subtracted.

Binding of Heparin to Fibrils Detected by Anisotropy Measurements. Binding of fluorescein-conjugated heparin to Tau/RNA fibrils was monitored in a Fluorolog 3 fluorometer equipped with automated dual polarizers (HORIBA Jobin Yvon) at an excitation wavelength of 480 nm and emission wavelength of 516 nm, with slitwidths set at 4 and 8 nm, respectively. The *G*-factor was determined according to $G = I_{HV}/I_{HH}$, where I_{HV} and I_{HH} are the vertically and horizontally polarized emissions when the sample is excited with horizontally polarized light. The anisotropy (r) was computed by the fluorometer software according to $r = (I_{VV} - GI_{VH})/(I_{VV} + 2GI_{VH})$.[37] Integration times were 0.1 s. Baseline anisotropy was measured with fluorescent heparin alone (in 100 mM NaCl, 10 mM HEPES, pH 7.4, buffered solution). Fibrils were then added to heparin for final concentrations of 6 μM Tau fibrils (monomer equivalents) and 40 nM heparin with a final volume of 500 μL. All measurements were performed at 37 °C.

Negative Stain Electron Microscopy (EM). To confirm the fibrillar nature of the Tau aggregates, 250-mesh carbon-coated copper grids were placed for 40 s onto 10 μM Tau protein, stained for 30 s with 2% uranyl acetate, and then air-dried on filter paper. The samples were examined with a Philips/FEI Tecnai-12 electron transmission microscope at 80 keV.

RESULTS

Tau Fibril Structure. A first step in the fibrillization of Tau is the formation of a multimeric nucleus.[20,38,39] In this step, negatively charged cofactors are thought to induce conformational changes in the intrinsically disordered Tau monomers[40] and to increase the local Tau concentration by simultaneously binding to multiple positively charged monomers.[25] We previously showed that fibrils formed in the presence of heparin assume a parallel, in-register β-sheet structure.[35,41] Since cofactors play a critical role in fibril nucleation, an important, yet unanswered, question is whether these auxiliary factors modulate overall fibril structure. In order to address this question, we first examined whether substitution of heparin by RNA affects β-strand arrangement and registry. For this purpose, six single-cysteine mutants of K18 and K19 (cysteines in positions 309, 310, 311, 317, 322, and 326) were labeled with the paramagnetic nitroxide label MTSL.[42] The sites were chosen to represent the stable core of the third microtubule binding repeat, which is critical for fibril formation.[43] Spin-labeled Tau was allowed to aggregate in the presence of RNA (polyA) for 3 days under agitation (see Materials and Methods). Continuous-wave EPR measurements produced single-line spectra for all fibrils (Figure 1A). The collapse of the three-line spectra that are normally observed for MTSL-labeled proteins can be explained by the exchange interaction between multiple spin labels. This is achieved by parallel, in-register arrangement of β-strands in which labels attached to identical positions in different Tau molecules are stacked along the fibril axis.[44] Fibrils formed in the presence of other RNA species such as polyU, double-stranded RNA (UA), tRNA, and whole yeast RNA extract produced similar results (Figure 1B). Also, different negatively charged polymers such as single-stranded DNA and polyglutamate produced fibrils that resulted in similar single-line characteristics (Figure 1C). Combined,

DOI: 10.1021/acs.biochem.5b00453
Biochemistry 2015, 54, 4731−4740

these data suggest that the parallel, in-register arrangement of β-strands is a common feature of Tau fibrils, independent of the cofactor that is used to induce aggregation.

Asymmetric Seeding Barrier. Despite the structural commonalities, packing interactions between β-sheets could vary substantially, resulting in different overall conformations. Indeed, K18 and K19 fibrils, both of which (in the presence of heparin) form parallel, in-register β-strands,[35] are conformationally distinct.[45] In order to gain further insights into the structure of RNA-induced fibrils, we next investigated their seeding properties. Since RNA interferes with the commonly used thioflavin assays of Tau fibril formation,[46] we chose an acrylodan-based fluorescence assay to monitor seeded fibril growth.[36] In this assay, acrylodan is attached to a single cysteine of the protein and fibril assembly is observed through the blueshift in the fluorescence emission maximum that occurs when the label moves from an aqueous environment in the disordered monomer to a hydrophobic environment in the folded fibril. First, K18 and K19 monomers were individually labeled at position 310 and mixed with their respective cysteine-free counterparts (molar ratio of 1:50). These mixtures were then combined with 10 mol % seeds (monomer equivalents) of K18 and K19. Samples were excited at 360 nm, and inverse emission maxima were plotted as a function of time (Figure 2). While K18 monomers grow onto K18 seeds, K19 monomers do not (Figure 2A). K19 seeds, however, facilitate growth of both K19 and K18 monomers, although the latter monomers grow less efficiently (Figure 2B). The data indicate that the previously observed asymmetric seeding barrier for heparin-mediated fibril growth is also preserved for fibrils formed in the presence of RNA. Furthermore, the data suggest that important structural properties of the fibrils are conserved.

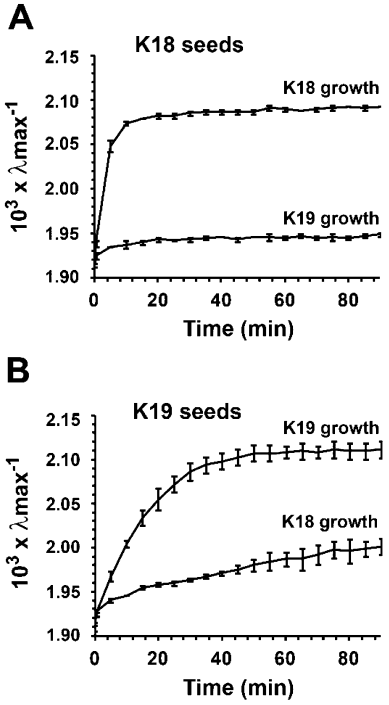

Figure 2. Seeding properties of 3R and 4R Tau. Tau fibril seeds (10% monomer equivalents) were mixed with monomers of K18 and K19 (98% cysteine free, 2% acrylodan labeled at position 310). As the labeled Tau monomers incorporate into the fibrils, the emission maxima shift to the blue. Inverse emission maxima plotted against time depict fibril growth: (A) K18 seeded growth and (B) K19 seeded growth. Values represent mean ± SD (n = 3 experiments). Tau concentration, 10 μM; cofactor, 20 μg/mL polyA RNA; excitation, 360 nm. An asymmetric seeding barrier prevents 3R Tau from growing onto 4R Tau seeds but not vice versa.

RNA Sustains Fibril Growth. Although it is clear that RNA is needed for nucleation, its role in fibril growth is not established. Here, we asked whether Tau fibril propagation could be sustained if RNA was omitted in consecutive cycles of seeding. The overall design of these experiments is outlined schematically in Figure 3A. Tau fibrils were first grown in a seeded reaction that included cofactor (cycle 1, Figure 3A). These fibrils were then sonicated and subjected to four consecutive cycles of seeding with cofactor either present or absent (cycle 2–5, Figure 3A). After each cycle, the samples were divided into two fractions: one for seed production via sonication and another for fibril sedimentation and SDS-PAGE analysis. The Coomassie-stained gels revealed that K18 and K19 fibrils propagated in the presence of RNA with similar amounts of fibril mass produced in each cycle (Figure 3B, left panels). When RNA was omitted during the elongation steps, fibril formation ceased (Figure 3B, right panels). The weak bands observed for cycles 2 and 3 (respective intensities of 24

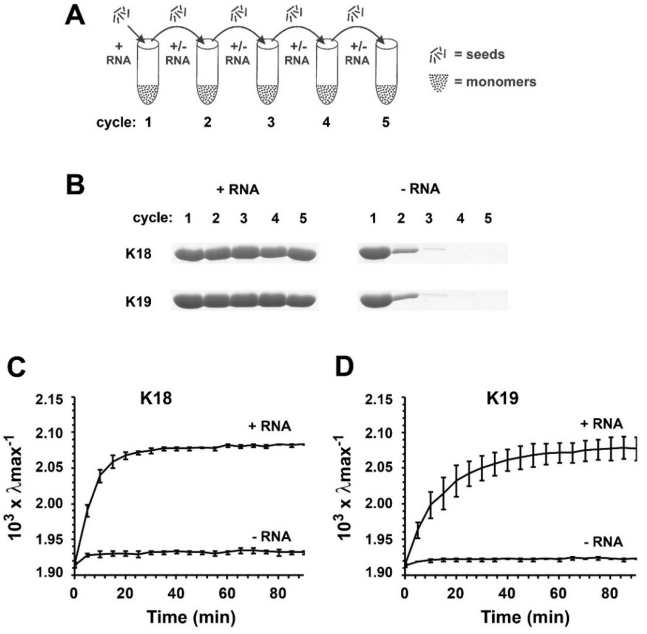

Figure 3. RNA sustains template-assisted fibril growth of 3R and 4R Tau. (A) Schematic diagram illustrating consecutive cycles of seeding and growth used in the experiment below. Beginning with cycle 2, RNA was omitted from all reactions. Only control experiments contained RNA throughout. After each cycle (24 h of growth at 22 °C), fibrils were sedimented by ultracentrifugation (100 000g) and analyzed by SDS-PAGE and Coomassie staining. (B) Fibril growth in the presence (left panel) and absence (right panel) of polyA RNA: upper panels, K18; lower panels, K19. Each reaction contained 10% seeds and 25 μM Tau. PolyA RNA, 125 μg/mL. (C, D) Tau fibril seeds (10% monomer equivalents) were mixed with K18 and K19 monomers (98% cysteine free, 2% acrylodan-labeled at position 310). (C) K18 growth onto K18 seeds in the presence and absence of RNA. (D) K19 growth onto K19 seeds in the presence and absence of RNA. The data demonstrate that RNA sustains template-assisted fibril growth.

DOI: 10.1021/acs.biochem.5b00453
Biochemistry 2015, 54, 4731−4740

and 2.0% for K18 and 24 and 2.1% for K19) are due to the seeds that were added to the reactions, and in the case of cycle 2, some residual aggregation as cofactor was carried over from cycle 1. The results demonstrate that RNA drives the amplification of Tau fibrils.

In order to gain additional support for cofactor-mediated fibril growth, we directly monitored the incorporation of Tau monomers into preformed fibrils using the acrylodan-based seeding assay from above. Specifically, K18 and K19 fibrils were formed in the presence of RNA and upon shearing were used as seeds for fibril propagation. In the presence of RNA, Tau monomers faithfully incorporated into the seeds (Figure 3C,D). These data agree with our previous observations (Figure 2) and are plotted for reference purposes only. Importantly, in the absence of RNA, no incorporation occurred (Figure 3C,D).

RNA Binding. Next, we asked whether RNA physically associates with Tau fibrils or whether the interactions are of transient nature. For this purpose, K18 and K19 fibrils were formed in the presence of polyA with 10% fibril seeds present to expedite aggregation. After sedimentation, the pellets were dissolved in buffer containing 2% SDS. The supernatants were adjusted to the same SDS concentration as that of the pellets. Absorption spectra were taken of the supernatant, the solubilized pellets, and control samples that contained RNA only (Figure 4A,C). The absorption maxima at 260 nm are

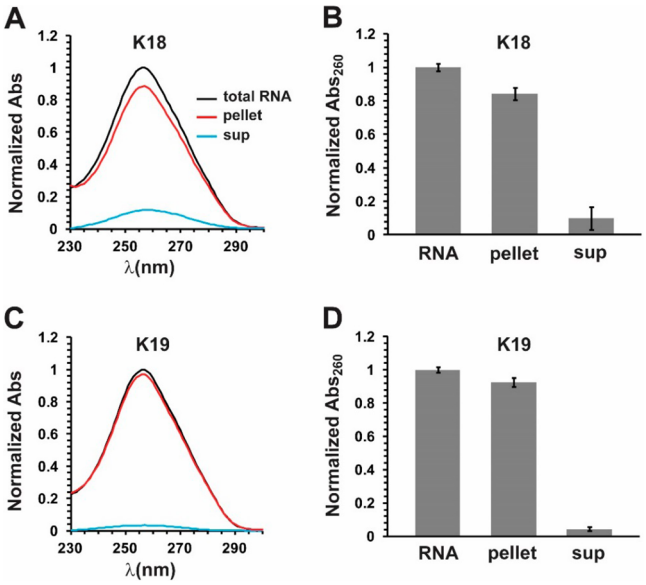

Figure 4. RNA binds to Tau fibrils. K18 and K19 fibrils were formed for 2 h at 37 °C from a mixture of Tau monomers (25 μM), respective seeds (10%), and polyA RNA (50 μg/mL). (A) Absorption spectra of solubilized K18 pellets (red), supernatants (blue), and total RNA (black). (B) Corresponding normalized intensities for experiments performed in triplicate. (C) Absorption spectra of solubilized K19 pellets, supernatant, and total RNA (color coding as above). (D) Corresponding normalized intensities for experiments performed in triplicate. Values represent mean ± SD. The data indicate that the majority of RNA is associated with K18 and K19 fibrils.

indicative of RNA. The protein itself has negligible absorbance at this wavelength, as it harbors only a single aromatic tyrosine. Quantification of three independent experiments for each K18 and K19 seeded growth reveals that the majority of RNA (~90%) became incorporated into the fibrils (Figure 4B,D). On the basis of the size distribution of RNA (0.2–2 kb), one RNA molecule bound to ~40–400 Tau molecules. Notably, dilution of Tau fibrils into buffer lacking RNA did not lead to the dissociation of Tau fibrils (Figure S1A). Furthermore, elevated concentrations of salt (500 mM NaCl) caused only minor dissociation of RNA (Figure S1B) and had no effect on fibril mass (Figure S1C). The findings suggest that RNA is firmly associated with the fibrils.

Cofactor Exchange. The question arose as to whether RNA/Tau fibril interactions could be perturbed by polyanions. We hypothesized that heparin, a polysulfonated glycosaminoglycan, might affect the interactions by competing for binding sites. In order to test this hypothesis, we added a 2-fold molar excess of heparin (based on the concentration of Tau monomers) to preformed K18/RNA fibrils. After incubation for 24 h at 37 °C, RNA had almost completely transferred into the supernatant (Figure 5A). The filamentous nature of K18 fibrils before and after the addition of heparin was verified by negative stain transmission electron microscopy (Figure 5B,C). Next, an equivalent set of experiments was carried out with K19 fibrils. Again, addition of heparin caused transfer of RNA into the supernatant (Figure 5D), although, in this case, transfer was less efficient. Importantly, in the absence of heparin, RNA was almost exclusively found in the pellet (Figure 4). The addition of heparin to K19/RNA fibrils did not affect the filamentous nature of the fibrils (compare Figure 5E with Figure 5F). The data indicate that heparin causes the release of RNA from Tau fibrils.

Since heparin does not absorb in the visible spectrum, it remained unclear whether heparin had replaced RNA on the fibril. To address this question, we added fluorescein-conjugated heparin to Tau/RNA fibrils and incubated the samples for 24 h at 37 °C. As before, pellets and supernatants were adjusted to the same volume containing 2% SDS (which solubilizes the fibrils). The absorbance at 260 nm revealed that the majority of RNA was released from K18 and K19 fibrils (Figure 6A,B). The results are similar to those obtained for nonconjugated heparin (Figure 5A,D), suggesting that the fluorescein modification and the change in average molecular weight (see Materials and Methods) did not affect the ability of heparin to release RNA from the Tau fibril cores. Notice that, again, the release of RNA from K19 fibrils was less efficient than that from K18 fibrils. This could reflect differences in RNA binding between the conformationally distinct fibrils. Specifically, some of the RNA binding sites in K19 fibrils might be in the interior rather than on the surface. Conjugated heparin was detected by measuring the absorbance at 490 nm. Importantly, the majority of heparin (~80%) associated with the K18 and K19 fibrils (Figure 6C,D). In both cases, the molar ratio of heparin to Tau was approximately 1:13.

In a last set of experiments, we sought to monitor heparin-to-fibril binding in real time. We reasoned that the tumbling of conjugated heparin would decrease as it bound to Tau fibrils. The fluorescence anisotropy of conjugated heparin was monitored as a function of time. The addition of K18/RNA and K19/RNA fibrils resulted in a steady increase in fluorescence anisotropy (Figure 6E,F), suggesting that the cofactor had associated with the fibrils. To ensure that the increase in anisotropy was not the result of heparin binding to residual K18 and K19 monomers, we monitored the anisotropy changes in the presence of K18 and K19 monomers alone. Only small increases in anisotropy were observed (Figure 6G,H). Combined, these findings demonstrate that heparin binds to Tau fibrils and replaces RNA on the fibril surface.

DOI: 10.1021/acs.biochem.5b00453
Biochemistry 2015, 54, 4731–4740

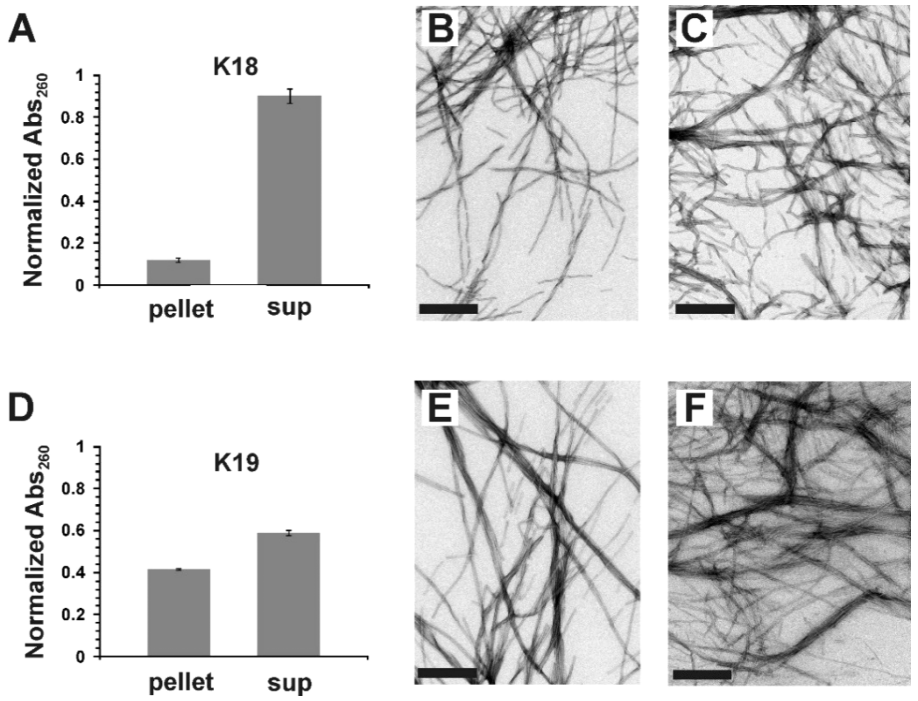

Figure 5. RNA dissociates from Tau fibrils. K18 and K19 fibrils (25 μM monomer added to 10% seeds) were grown in the presence of RNA (50 μg/mL) and subsequently incubated for 24 h with heparin (50 μM). (A) Normalized absorbance at 260 nm for solubilized K18 pellet and supernatant. (B) K18/RNA fibrils. (C) K18/heparin fibrils after heparin/RNA exchange. (D) Normalized absorbance at 260 nm for solubilized K19 pellet and supernatant. (E) K19/RNA fibrils. (F) K19/heparin fibrils after heparin/RNA exchange. Intensities represent mean ± SD (n = 3 experiments). Bar, 400 nm. The data suggest that heparin replaces the majority of RNA that is bound to K18 and K19 fibrils.

DISCUSSION

Neurofibrillary lesions composed of the microtubule associated protein Tau are a defining hallmark of Alzheimer disease and other Tauopathies. Although RNA was already identified in the late 90s to be a major nonproteinaceous component of these lesions[33,34] and was shown to stimulate Tau fibril formation *in vitro*,[25,26] it remained unknown whether RNA physically associates with Tau fibrils. In this study, we investigated the RNA/Tau interaction and examined the effects of RNA on fibril conformation and growth.

We observed that fibrils formed in the presence of different RNA species (as well as DNA and polyglutamate) assume a parallel, in-register arrangement of β-strands. This structure was previously observed for Tau fibrils formed in the presence of heparin,[35] suggesting that the strand arrangement is a conserved property of Tau fibrils that is not modulated by inducers. We furthermore identified an asymmetric seeding barrier in which 4R Tau grows onto 3R Tau seeds but not vice versa. The existence of a similar barrier for RNA- (this study) and heparin-induced Tau fibrils[36] indicates that the lateral associations between β-sheets in these fibrils are similar. The findings are remarkable considering that the nucleating agents are molecularly distinct and that Tau monomers exhibit a high degree of conformational plasticity.[36,47] They suggest that two key features of the fibril structure are preserved: (1) strand arrangement, which reflects interactions parallel to the long fibril axis, and (2) β-sheet packing, which reflects interactions perpendicular to the fibril axis. However, since differently packed conformers in an ensemble of 4R Tau fibrils could produce the same seeding barrier,[45,48] the relative populations of conformers could vary in a cofactor-dependent manner.

Our experiments on template-assisted growth demonstrate that RNA is required for the recruitment of Tau monomers onto seeds. The specific role RNA plays in this process remains unclear. Although Tau monomers are intrinsically disordered, long-range interactions within the protein could lower the accessibility to the repeats and hence prevent docking of the monomers to the fibril ends. Specifically, it has been recognized that the N- and C-termini of Tau might interact with residues in the third microtubule binding repeat. These interactions produce discontinuous epitopes that are recognized by the antibodies Alz-50 and MC-1.[49] Further support for this double-hairpin (or paperclip) model was provided by FRET measurements in which donor and acceptor fluorophores in the repeats and in the termini came into close proximity.[17] NMR experiments provided a refined model in which an intricate network of transient long-range interactions establishes a dynamic structural ensemble of loosely packed Tau monomers.[50] The binding of cofactors could have a direct effect on these ensembles. In support of this, heparin was observed to compact the microtubule binding domain and to break long-range interactions that could prevent sampling of aggregation-competent conformers.[51] However, since in the current study only truncated Tau, which lacks the N- and C-termini, was used, it is unlikely that conformational changes alone can explain the cofactor dependence on growth. Alternatively, the cofactor could lower the activation barrier of docking, allowing positively charged side chains in the repeat region to stack. Additionally, the cofactor could stabilize the growing fibril by directly binding to its surface. In support of this, we found that RNA associates with fibrils.

If RNA molecules bound parallel to the long fibril axis, as has been proposed for heparin,[52] then a single nucleic acid molecule, depending on polymer length, could associate with

DOI: 10.1021/acs.biochem.5b00453
Biochemistry 2015, 54, 4731−4740

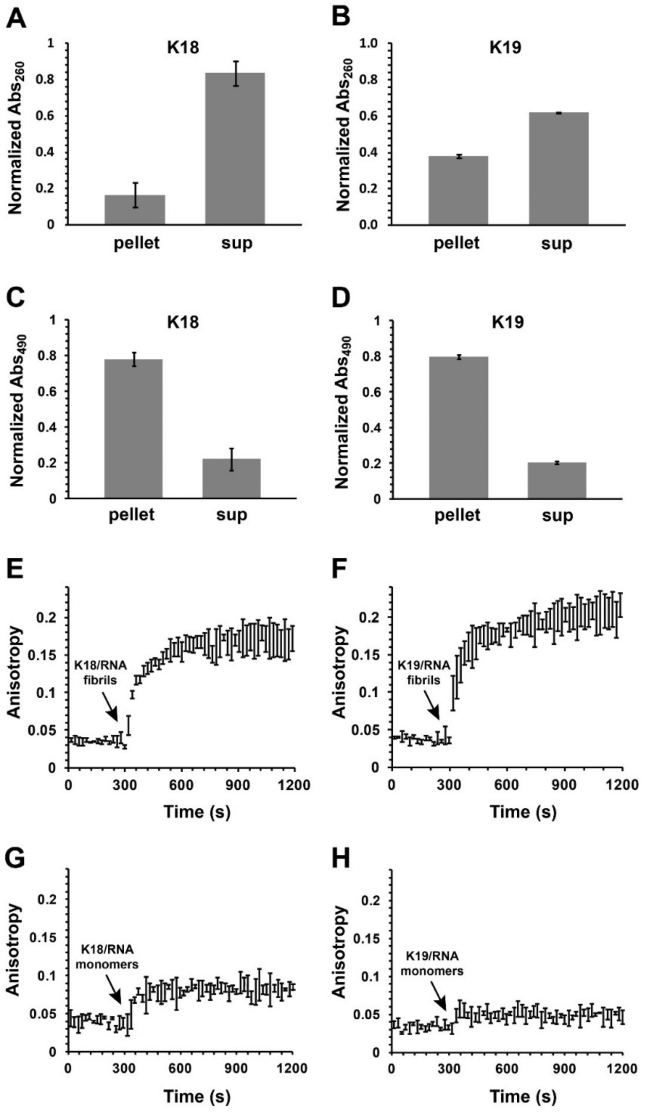

Figure 6. Heparin replaces RNA on Tau fibrils. K18 and K19 fibrils (25 μM monomer added to 10% seeds) were grown in the presence of RNA (50 μg/mL) and subsequently incubated for 24 h with fluorescein-conjugated heparin (2.5 μM). (A, B) Normalized absorbance at 260 nm for solubilized K18 and K19 pellets and supernatants. (C, D) Normalized absorbance at 490 nm for solubilized K18 and K19 pellets and supernatants. (E, F) Fluorescence anisotropy changes upon association of heparin with K18/RNA and K19/RNA fibrils. (G, H) Fluorescence anisotropy changes upon association of heparin with K18/RNA and K19/RNA monomers. Tau concentration, 6 μM; heparin concentration, 40 nM; excitation, 480 nm; emission, 516 nm. Arrows mark additions of Tau fibrils or Tau monomers to fluorescein-conjugated heparin. The large changes in fluorescence anisotropy observed in E and F imply that heparin binds to Tau fibrils.

tens or hundreds of layers of Tau proteins. This could compensate the charge repulsions between protruding lysines that are stacked in the parallel, in-register structure of the fibril. Even minor (substoichiometric) incorporation of cofactors[12,38,53] could hence result in major reinforcement of the fibril structure. Importantly, a fibril-stabilizing function of cofactor has recently been observed for heparin.[54] The specific effects cofactors assert on fibril stability are most likely dependent on polymer length and type. Whether cofactor is needed to stabilize Tau fibrils could also be dependent on conformation. Indeed, the Tau disease mutant ΔK280,[55] which forms fibrils that are structurally distinct from those of wild-type Tau,[56] does not require cofactor for fibrillization.[12]

Regardless of the stabilizing role of cofactors, the decoration of Tau fibrils with nonproteinacious molecules could encode important biological information. The nature of the cofactor on the surface of the fibril could influence how the fibril interacts with cellular components. The uptake of Tau fibrils, for example, is, at least in part, mediated by heparan sulfate proteoglycans (HSPGs).[57] The efficiency of this process could depend on the accessibility of binding sites and the particular nature of the cofactors that decorate the fibril. We observed that heparin replaces RNA on the fibril surface. A similar mechanism could facilitate fibril binding to HSPGs on the cell surface. Exchangeable cofactors on the surface of Tau fibrils may enhance fibril transmission between neurons, whereas nonexchangeable ones may inhibit it. A new intricate model emerges in which cofactors not only sustain template-assisted growth but also are part of the fibril structure (Figure 7). In

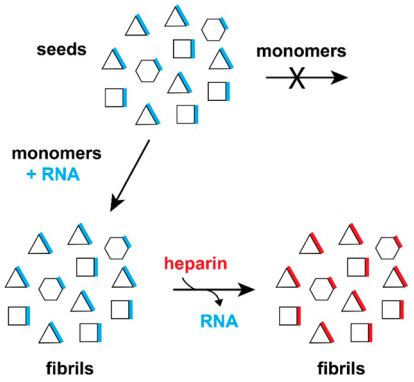

Figure 7. Schematic model for cofactor participation in Tau fibril growth and decoration. RNA (blue) not only sustains template-assisted growth but also decorates the fibril surface. Heparin (red) can substitute RNA on the surface and thereby change the properties of the fibril. Different conformers of Tau fibrils (squares, triangles, and hexagons) will have distinct associations. The decoration of Tau fibrils with other cofactors (not shown) could produce a complex structural ensemble with diverse biological activities.

some fibrils, cofactors may be not only bound to the surface but also incorporated into the amyloidogenic core. The K19 fibrils that were characterized in this study may be one example. In these fibrils, a significant population of RNA molecules could not be replaced by heparin (Figures 5 and 6).

The molecular species that decorate the surface of Tau fibrils *in vivo* may depend on multiple factors including fibril conformation, localization, cell type, and metabolic state. It is notable that approximately 20% of the Tau lesions in the hippocampal and entorhinal regions of Alzheimer disease brain does not contain RNA.[33] Associations with other cofactors[58−61] are a plausible explanation.

The template-assisted conversion of Tau exhibits remarkable similarities to the conversion of prion proteins,[62,63] where RNA,[64,65] HSPGs,[66] lipids,[67,68] and combinations of cofactors[68,69] are found to stimulate conformational transitions. These similarities underscore common molecular mechanisms in the propagation of the misfolded species. A detailed understanding of the Tau/cofactor interactions and their biological consequences could be critical for interfering with the intracerebral spreading of Tau pathology.

DOI: 10.1021/acs.biochem.5b00453
Biochemistry 2015, 54, 4731−4740

■ ASSOCIATED CONTENT

Supporting Information

Figure S1: RNA/Tau fibril interactions at elevated salt concentrations and stability of Tau fibrils upon limited dilution. The Supporting Information is available free of charge on the ACS Publications website at DOI: 10.1021/acs.biochem.5b00453.

■ AUTHOR INFORMATION

Corresponding Author

*Tel: (303) 871-4135. Fax: (303) 871-2254. E-mail: martin.margittai@du.edu.

Funding

This project was supported by NIH/NINDS grant no. R01NS076619 (to M.M.).

Notes

The authors declare no competing financial interest.

■ REFERENCES

(1) Buee, L., Bussiere, T., Buee-Scherrer, V., Delacourte, A., and Hof, P. R. (2000) Tau protein isoforms, phosphorylation and role in neurodegenerative disorders. *Brain Res. Rev. 33*, 95−130.

(2) Braak, H., and Braak, E. (1991) Neuropathological stageing of Alzheimer-related changes. *Acta Neuropathol. 82*, 239−259.

(3) Braak, H., Alafuzoff, I., Arzberger, T., Kretzschmar, H., and Del Tredici, K. (2006) Staging of Alzheimer disease-associated neurofibrillary pathology using paraffin sections and immunocytochemistry. *Acta Neuropathol. 112*, 389−404.

(4) Liu, L., Drouet, V., Wu, J. W., Witter, M. P., Small, S. A., Clelland, C., and Duff, K. (2012) Trans-synaptic spread of tau pathology in vivo. *PLoS One 7*, e31302.

(5) de Calignon, A., Polydoro, M., Suarez-Calvet, M., William, C., Adamowicz, D. H., Kopeikina, K. J., Pitstick, R., Sahara, N., Ashe, K. H., Carlson, G. A., Spires-Jones, T. L., and Hyman, B. T. (2012) Propagation of tau pathology in a model of early Alzheimer's disease. *Neuron 73*, 685−697.

(6) Dujardin, S., Lecolle, K., Caillierez, R., Begard, S., Zommer, N., Lachaud, C., Carrier, S., Dufour, N., Auregan, G., Winderickx, J., Hantraye, P., Deglon, N., Colin, M., and Buee, L. (2014) Neuron-to-neuron wild-type Tau protein transfer through a trans-synaptic mechanism: relevance to sporadic tauopathies. *Acta Neuropathol. Commun. 2*, 14.

(7) Kfoury, N., Holmes, B. B., Jiang, H., Holtzman, D. M., and Diamond, M. I. (2012) Trans-cellular Propagation of Tau Aggregation by Fibrillar Species. *J. Biol. Chem. 287*, 19440−19451.

(8) Goedert, M., Spillantini, M. G., Cairns, N. J., and Crowther, R. A. (1992) Tau proteins of Alzheimer paired helical filaments: abnormal phosphorylation of all six brain isoforms. *Neuron 8*, 159−168.

(9) Spillantini, M. G., and Goedert, M. (2013) Tau pathology and neurodegeneration. *Lancet Neurol. 12*, 609−622.

(10) Wischik, C. M., Novak, M., Thogersen, H. C., Edwards, P. C., Runswick, M. J., Jakes, R., Walker, J. E., Milstein, C., Roth, M., and Klug, A. (1988) Isolation of a fragment of tau derived from the core of the paired helical filament of Alzheimer disease. *Proc. Natl. Acad. Sci. U. S. A. 85*, 4506−4510.

(11) Novak, M., Kabat, J., and Wischik, C. M. (1993) Molecular characterization of the minimal protease resistant tau unit of the Alzheimer's disease paired helical filament. *EMBO J. 12*, 365−370.

(12) von Bergen, M., Barghorn, S., Muller, S. A., Pickhardt, M., Biernat, J., Mandelkow, E. M., Davies, P., Aebi, U., and Mandelkow, E. (2006) The core of tau-paired helical filaments studied by scanning transmission electron microscopy and limited proteolysis. *Biochemistry 45*, 6446−6457.

(13) Wischik, C. M., Novak, M., Edwards, P. C., Klug, A., Tichelaar, W., and Crowther, R. A. (1988) Structural characterization of the core of the paired helical filament of Alzheimer disease. *Proc. Natl. Acad. Sci. U. S. A. 85*, 4884−4888.

(14) Wegmann, S., Medalsy, I. D., Mandelkow, E., and Muller, D. J. (2013) The fuzzy coat of pathological human Tau fibrils is a two-layered polyelectrolyte brush. *Proc. Natl. Acad. Sci. U. S. A. 110*, E313−321.

(15) Gustke, N., Trinczek, B., Biernat, J., Mandelkow, E. M., and Mandelkow, E. (1994) Domains of tau protein and interactions with microtubules. *Biochemistry 33*, 9511−9522.

(16) Barghorn, S., and Mandelkow, E. (2002) Toward a unified scheme for the aggregation of tau into Alzheimer paired helical filaments. *Biochemistry 41*, 14885−14896.

(17) Jeganathan, S., von Bergen, M., Brutlach, H., Steinhoff, H. J., and Mandelkow, E. (2006) Global hairpin folding of tau in solution. *Biochemistry 45*, 2283−2293.

(18) von Bergen, M., Barghorn, S., Li, L., Marx, A., Biernat, J., Mandelkow, E. M., and Mandelkow, E. (2001) Mutations of tau protein in frontotemporal dementia promote aggregation of paired helical filaments by enhancing local beta-structure. *J. Biol. Chem. 276*, 48165−48174.

(19) Berriman, J., Serpell, L. C., Oberg, K. A., Fink, A. L., Goedert, M., and Crowther, R. A. (2003) Tau filaments from human brain and from in vitro assembly of recombinant protein show cross-beta structure. *Proc. Natl. Acad. Sci. U. S. A. 100*, 9034−9038.

(20) Friedhoff, P., von Bergen, M., Mandelkow, E. M., Davies, P., and Mandelkow, E. (1998) A nucleated assembly mechanism of Alzheimer paired helical filaments. *Proc. Natl. Acad. Sci. U. S. A. 95*, 15712−15717.

(21) Goedert, M., Jakes, R., Spillantini, M. G., Hasegawa, M., Smith, M. J., and Crowther, R. A. (1996) Assembly of microtubule-associated protein tau into Alzheimer-like filaments induced by sulphated glycosaminoglycans. *Nature 383*, 550−553.

(22) Perez, M., Valpuesta, J. M., Medina, M., Montejo de Garcini, E., and Avila, J. (1996) Polymerization of tau into filaments in the presence of heparin: the minimal sequence required for tau-tau interaction. *J. Neurochem. 67*, 1183−1190.

(23) Wilson, D. M., and Binder, L. I. (1997) Free fatty acids stimulate the polymerization of tau and amyloid beta peptides. In vitro evidence for a common effector of pathogenesis in Alzheimer's disease. *Am. J. Pathol. 150*, 2181−2195.

(24) King, M. E., Ahuja, V., Binder, L. I., and Kuret, J. (1999) Ligand-dependent tau filament formation: implications for Alzheimer's disease progression. *Biochemistry 38*, 14851−14859.

(25) Kampers, T., Friedhoff, P., Biernat, J., Mandelkow, E. M., and Mandelkow, E. (1996) RNA stimulates aggregation of microtubule-associated protein tau into Alzheimer-like paired helical filaments. *FEBS Lett. 399*, 344−349.

(26) Hasegawa, M., Crowther, R. A., Jakes, R., and Goedert, M. (1997) Alzheimer-like changes in microtubule-associated protein Tau induced by sulfated glycosaminoglycans. Inhibition of microtubule binding, stimulation of phosphorylation, and filament assembly depend on the degree of sulfation. *J. Biol. Chem. 272*, 33118−33124.

(27) Crowther, R. A., Olesen, O. F., Jakes, R., and Goedert, M. (1992) The microtubule binding repeats of tau protein assemble into filaments like those found in Alzheimer's disease. *FEBS Lett. 309*, 199−202.

(28) Crowther, R. A., Olesen, O. F., Smith, M. J., Jakes, R., and Goedert, M. (1994) Assembly of Alzheimer-like filaments from full-length tau protein. *FEBS Lett. 337*, 135−138.

(29) Bramblett, G. T., Goedert, M., Jakes, R., Merrick, S. E., Trojanowski, J. Q., and Lee, V. M. (1993) Abnormal tau phosphorylation at Ser396 in Alzheimer's disease recapitulates development and contributes to reduced microtubule binding. *Neuron 10*, 1089−1099.

(30) Biernat, J., Gustke, N., Drewes, G., Mandelkow, E. M., and Mandelkow, E. (1993) Phosphorylation of Ser262 strongly reduces binding of tau to microtubules: distinction between PHF-like immunoreactivity and microtubule binding. *Neuron 11*, 153−163.

DOI: 10.1021/acs.biochem.5b00453
Biochemistry 2015, 54, 4731−4740

(31) Li, L., von Bergen, M., Mandelkow, E. M., and Mandelkow, E. (2002) Structure, stability, and aggregation of paired helical filaments from tau protein and FTDP-17 mutants probed by tryptophan scanning mutagenesis. *J. Biol. Chem. 277*, 41390−41400.
(32) Patrick, G. N., Zukerberg, L., Nikolic, M., de la Monte, S., Dikkes, P., and Tsai, L. H. (1999) Conversion of p35 to p25 deregulates Cdk5 activity and promotes neurodegeneration. *Nature 402*, 615−622.
(33) Ginsberg, S. D., Crino, P. B., Lee, V. M., Eberwine, J. H., and Trojanowski, J. Q. (1997) Sequestration of RNA in Alzheimer's disease neurofibrillary tangles and senile plaques. *Ann. Neurol. 41*, 200−209.
(34) Ginsberg, S. D., Galvin, J. E., Chiu, T. S., Lee, V. M., Masliah, E., and Trojanowski, J. Q. (1998) RNA sequestration to pathological lesions of neurodegenerative diseases. *Acta Neuropathol. 96*, 487−494.
(35) Siddiqua, A., and Margittai, M. (2010) Three- and four-repeat Tau coassemble into heterogeneous filaments: an implication for Alzheimer disease. *J. Biol. Chem. 285*, 37920−37926.
(36) Dinkel, P. D., Siddiqua, A., Huynh, H., Shah, M., and Margittai, M. (2011) Variations in Filament Conformation Dictate Seeding Barrier between Three- and Four-Repeat Tau. *Biochemistry 50*, 4330−4336.
(37) Lakowicz, J. R. (2006) *Principles of Fluorescence Spectroscopy*, 3rd ed., pp 353−382, Springer, New York.
(38) Ramachandran, G., and Udgaonkar, J. B. (2011) Understanding the kinetic roles of the inducer heparin and of rod-like protofibrils during amyloid fibril formation by Tau protein. *J. Biol. Chem. 286*, 38948−38959.
(39) Ramachandran, G., and Udgaonkar, J. B. (2012) Evidence for the existence of a secondary pathway for fibril growth during the aggregation of tau. *J. Mol. Biol. 421*, 296−314.
(40) Kuret, J., Congdon, E. E., Li, G., Yin, H., Yu, X., and Zhong, Q. (2005) Evaluating triggers and enhancers of tau fibrillization. *Microsc. Res. Tech. 67*, 141−155.
(41) Margittai, M., and Langen, R. (2004) Template-assisted filament growth by parallel stacking of tau. *Proc. Natl. Acad. Sci. U. S. A. 101*, 10278−10283.
(42) Berliner, L. J., Grunwald, J., Hankovszky, H. O., and Hideg, K. (1982) A novel reversible thiol-specific spin label: papain active site labeling and inhibition. *Anal. Biochem. 119*, 450−455.
(43) von Bergen, M., Friedhoff, P., Biernat, J., Heberle, J., Mandelkow, E. M., and Mandelkow, E. (2000) Assembly of tau protein into Alzheimer paired helical filaments depends on a local sequence motif ((306)VQIVYK(311)) forming beta structure. *Proc. Natl. Acad. Sci. U. S. A. 97*, 5129−5134.
(44) Margittai, M., and Langen, R. (2008) Fibrils with parallel in-register structure constitute a major class of amyloid fibrils: molecular insights from electron paramagnetic resonance spectroscopy. *Q. Rev. Biophys. 41*, 265−297.
(45) Siddiqua, A., Luo, Y., Meyer, V., Swanson, M. A., Yu, X., Wei, G., Zheng, J., Eaton, G. R., Ma, B., Nussinov, R., Eaton, S. S., and Margittai, M. (2012) Conformational basis for asymmetric seeding barrier in filaments of three- and four-repeat tau. *J. Am. Chem. Soc. 134*, 10271−10278.
(46) Friedhoff, P., Schneider, A., Mandelkow, E. M., and Mandelkow, E. (1998) Rapid assembly of Alzheimer-like paired helical filaments from microtubule-associated protein tau monitored by fluorescence in solution. *Biochemistry 37*, 10223−10230.
(47) Frost, B., Ollesch, J., Wille, H., and Diamond, M. I. (2009) Conformational diversity of wild-type Tau fibrils specified by templated conformation change. *J. Biol. Chem. 284*, 3546−3551.
(48) Yu, X., Luo, Y., Dinkel, P., Zheng, J., Wei, G., Margittai, M., Nussinov, R., and Ma, B. (2012) Cross-seeding and conformational selection between three- and four-repeat human Tau proteins. *J. Biol. Chem. 287*, 14950−14959.
(49) Jicha, G. A., Bowser, R., Kazam, I. G., and Davies, P. (1997) Alz-50 and MC-1, a new monoclonal antibody raised to paired helical filaments, recognize conformational epitopes on recombinant tau. *J. Neurosci. Res. 48*, 128−132.
(50) Mukrasch, M. D., Bibow, S., Korukottu, J., Jeganathan, S., Biernat, J., Griesinger, C., Mandelkow, E., and Zweckstetter, M. (2009) Structural polymorphism of 441-residue tau at single residue resolution. *PLoS Biol. 7*, e34.
(51) Elbaum-Garfinkle, S., and Rhoades, E. (2012) Identification of an aggregation-prone structure of tau. *J. Am. Chem. Soc. 134*, 16607−16613.
(52) Sibille, N., Sillen, A., Leroy, A., Wieruszeski, J. M., Mulloy, B., Landrieu, I., and Lippens, G. (2006) Structural impact of heparin binding to full-length Tau as studied by NMR spectroscopy. *Biochemistry 45*, 12560−12572.
(53) Carlson, S. W., Branden, M., Voss, K., Sun, Q., Rankin, C. A., and Gamblin, T. C. (2007) A complex mechanism for inducer mediated tau polymerization. *Biochemistry 46*, 8838−8849.
(54) Luo, Y., Dinkel, P., Yu, X., Margittai, M., Zheng, J., Nussinov, R., Wei, G., and Ma, B. (2013) Molecular insights into the reversible formation of tau protein fibrils. *Chem. Commun. (Cambridge, U. K.) 49*, 3582−3584.
(55) Rizzu, P., Van Swieten, J. C., Joosse, M., Hasegawa, M., Stevens, M., Tibben, A., Niermeijer, M. F., Hillebrand, M., Ravid, R., Oostra, B. A., Goedert, M., van Duijn, C. M., and Heutink, P. (1999) High prevalence of mutations in the microtubule-associated protein tau in a population study of frontotemporal dementia in the Netherlands. *Am. J. Hum. Genet. 64*, 414−421.
(56) Meyer, V., Dinkel, P. D., Luo, Y., Yu, X., Wei, G., Zheng, J., Eaton, G. R., Ma, B., Nussinov, R., Eaton, S. S., and Margittai, M. (2014) Single mutations in tau modulate the populations of fibril conformers through seed selection. *Angew. Chem., Int. Ed. 53*, 1590−1593.
(57) Holmes, B. B., Devos, S. L., Kfoury, N., Li, M., Jacks, R., Yanamandra, K., Ouidja, M. O., Brodsky, F. M., Marasa, J., Bagchi, D. P., Kotzbauer, P. T., Miller, T. M., Papy-Garcia, D., and Diamond, M. I. (2013) Heparan sulfate proteoglycans mediate internalization and propagation of specific proteopathic seeds. *Proc. Natl. Acad. Sci. U. S. A. 110*, E3138−3147.
(58) Perry, G., Siedlak, S. L., Richey, P., Kawai, M., Cras, P., Kalaria, R. N., Galloway, P. G., Scardina, J. M., Cordell, B., Greenberg, B. D., et al. (1991) Association of heparan sulfate proteoglycan with the neurofibrillary tangles of Alzheimer's disease. *J. Neurosci. 11*, 3679−3683.
(59) Snow, A. D., Mar, H., Nochlin, D., Kresse, H., and Wight, T. N. (1992) Peripheral distribution of dermatan sulfate proteoglycans (decorin) in amyloid-containing plaques and their presence in neurofibrillary tangles of Alzheimer's disease. *J. Histochem. Cytochem. 40*, 105−113.
(60) Su, J. H., Cummings, B. J., and Cotman, C. W. (1992) Localization of heparan sulfate glycosaminoglycan and proteoglycan core protein in aged brain and Alzheimer's disease. *Neuroscience 51*, 801−813.
(61) DeWitt, D. A., Silver, J., Canning, D. R., and Perry, G. (1993) Chondroitin sulfate proteoglycans are associated with the lesions of Alzheimer's disease. *Exp. Neurol. 121*, 149−152.
(62) Prusiner, S. B. (1998) Prions. *Proc. Natl. Acad. Sci. U. S. A. 95*, 13363−13383.
(63) Collinge, J., and Clarke, A. R. (2007) A general model of prion strains and their pathogenicity. *Science 318*, 930−936.
(64) Deleault, N. R., Lucassen, R. W., and Supattapone, S. (2003) RNA molecules stimulate prion protein conversion. *Nature 425*, 717−720.
(65) Deleault, N. R., Harris, B. T., Rees, J. R., and Supattapone, S. (2007) Formation of native prions from minimal components in vitro. *Proc. Natl. Acad. Sci. U. S. A. 104*, 9741−9746.
(66) Deleault, N. R., Geoghegan, J. C., Nishina, K., Kascsak, R., Williamson, R. A., and Supattapone, S. (2005) Protease-resistant prion protein amplification reconstituted with partially purified substrates and synthetic polyanions. *J. Biol. Chem. 280*, 26873−26879.
(67) Deleault, N. R., Piro, J. R., Walsh, D. J., Wang, F., Ma, J., Geoghegan, J. C., and Supattapone, S. (2012) Isolation of phosphatidylethanolamine as a solitary cofactor for prion formation

DOI: 10.1021/acs.biochem.5b00453
Biochemistry 2015, 54, 4731−4740

in the absence of nucleic acids. *Proc. Natl. Acad. Sci. U. S. A. 109*, 8546−8551.
(68) Deleault, N. R., Walsh, D. J., Piro, J. R., Wang, F., Wang, X., Ma, J., Rees, J. R., and Supattapone, S. (2012) Cofactor molecules maintain infectious conformation and restrict strain properties in purified prions. *Proc. Natl. Acad. Sci. U. S. A. 109*, E1938−1946.
(69) Wang, F., Wang, X., Yuan, C. G., and Ma, J. (2010) Generating a prion with bacterially expressed recombinant prion protein. *Science 327*, 1132−1135.

DOI: 10.1021/acs.biochem.5b00453
Biochemistry 2015, 54, 4731−4740